Desalination and Water Treatment
www.deswater.com

doi: 10.1080/19443994.2015.1072741

57 (2016) 15397–15409
July

Taylor & Francis
Taylor & Francis Group

Synthesis and characterization of nanoporous silica SBA-15 diaminocyclohexane and its application in removal of Cu(II) and Ni(II) from aqueous solution

Bhogineni Sreenu[a], Priti Sharma[b], Kalluru Seshaiah[a,*], A.P. Singh[b]

[a]*Department of Chemistry, Inorganic and Analytical Division, Sri Venkateswara University, Tirupati, AP 517502, India, email: srinubhogineni@gmail.com (B. Sreenu), Tel./Fax: +918772248499; email: seshaiahsvu@yahoo.co.in (K. Seshaiah)*
[b]*Catalysis Division, National Chemical Laboratory, Pune, India, emails: priti.sharma55@gmail.com (P. Sharma), ap.singh@ncl.res.in (A.P. Singh)*

Received 29 November 2014; Accepted 5 July 2015

ABSTRACT

A new nanoporous 1,2-diaminocyclohexane-functionalized SBA-15 (Dach@SBA-15) silica sorbent was prepared. The structure and physicochemical properties of the material were characterized by elemental analysis, X-ray diffraction, transmission electron microscopy (TEM), scanning electron microscopy, FT-IR spectroscopy, nitrogen adsorption–desorption isotherms and thermogravimetric analysis. TEM image clearly showed the sheet-like structure of Dach@SBA-15. The organic functional groups were successfully grafted onto the SBA-15 surface and the ordering of the support was not affected by the chemical modification. The Dach@SBA-15was used as a sorbent for removal of Cu(II) and Ni(II) from aqueous solution. Experimental parameters like effect of pH, contact time and metal ion concentration were studied and optimized. The adsorption isotherm data fitted well to Langmuir isotherm model and the monolayer adsorption capacity values for Cu(II) was 90.09 and for Ni (II) was 84.03 mg/g at 303 K. The experimental kinetic data fitted very well to the pseudo-second-order model. The Dach@SBA-15 could be used as a sorbent for removal of Cu(II) and Ni(II) from aqueous medium.

Keywords: Nanoporous silica; Heavy metals; Adsorption; FT-IR; BET; FAAS

1. Introduction

Heavy metal contamination of water resources has become an environmental concern in both developing and developed countries. The massive urbanization and industrial growth are the major causes for the presence of heavy metals in different segments of the environment, air, water, soil and biosphere [1]. The industrial effluents which contain different derivatives of heavy metals, such as arsenic, copper, cadmium, chromium, nickel, lead, mercury and zinc, which are persistent and non-biodegradable, are continuously discharged into the environment producing significant effects on aquatic environment [2–5]. Among the heavy metals, nickel and copper are especially toxic to living organisms. Several industrial activities like mineral processing, electroplating, production of paints and batteries, manufacturing of sulphate, porcelain enamelling, electric boards/circuits manufacturing industries as well as agriculture sector including

*Corresponding author.

fertilizers, pesticides are responsible for generating wastewater containing nickel and copper ions [6]. World Health Organization has recommended a maximum acceptable limit of 0.02 mg/L for Ni(II) and 1.5 mg/L for Cu(II) in drinking water [7]. The Ni(II) and Cu(II) cause asthma, lung cancer, renal and hepatic damage, severe mucosal irritation, wide spread capillary damage, gastrointestinal irritation and possibly necrotic changes in kidney and liver [8].

Removal of heavy metals from water and wastewater has become a major challenge for scientists. Various methods used for the removal of heavy metal ions from wastewater include precipitation, ion exchange, reverse osmosis, membrane filtration, flotation, solvent extraction and coagulation [9–14]. However, these techniques are not economically viable due to higher maintenance and operational costs. Moreover, adsorption technology is most promising low expensive and environmentally benign in the removal of toxic heavy metal ions from wastewater [15]. Recently, application of various adsorbents like activated carbon nanotubes [16], zeolites [17], resins [18], clays [19], biomaterials [20], rice husk ash and neem bark [21], grape stalk wastes [22] and nanoporous silica [23] in removal of heavy metals has been studied. Among these materials, nanoporous silica functionalized with various organic materials is increasingly utilized as an adsorbent because of its high selectivity and chemical stability for heavy metal ions adsorption [24]. The nanoporous SBA-15 sorbents are useful in removal of heavy metal ions from environmental samples [25]. The adsorption capacity and selectivity of nanoporous SBA-15 sorbents mainly depend on the surface modification of material by organic functionalization consisting of oxygen, nitrogen and sulphur atoms that can act as coordinate sites for metal ions [26,27].

In the present study, we have synthesized a hybrid sorbent by functionalizing a nanoporous SBA-15 with 1,2-diaminocyclohexane (Dach@SBA-15). The sorbent was characterized by elemental analysis, X-ray diffraction (XRD),transmission electron microscopy (TEM), scanning electron microscopy (SEM), FT-IR spectroscopy, nitrogen adsorption–desorption isotherms and thermogravimetric analysis (TGA). The 1,2-diaminocyclohexane-functionalized SBA-15 was used as adsorbent for the removal of heavy metal ions, Cu(II) and Ni(II) from aqueous medium. The experimental factors such as pH, concentration of initial metal ion, contact time and adsorbent dose were studied in order to optimize the experimental conditions for application of Dach@SBA-15 as sorbent in removal of Cu(II) and Ni (II) from aqueous medium. The adsorption isotherm data were analysed using Langmuir and Freundlich models and found that the data were fitted well to Langmuir isotherm model and the monolayer adsorption capacity values were found to be 90.09 for Cu(II) and 84.03 mg/g for Ni(II) at 303 K. The experimental kinetic data fitted very well with the pseudo-second-order model.

2. Experimental

2.1. Chemicals

Poly (ethylene glycol)block-poly (propylene glycol) block-poly (ethylene glycol) (pluronic P123 $EO_{20}PO_{70}EO_{20}$, Mw = 5,800), TEOS (tetra ethylorthosilicate), 3-chloropropyltrimethoxy silane and 1,2-diaminocyclohexane were purchased from Aldrich. Copper sulphate, nickel chloride hexa hydrate, dichloromethane (DCM) hydrochloride acid 35% and nitric acid were used in the studies. ACS reagent grade HCl, NaOH and buffer solutions (E. Merck) were used to adjust the solution pH. The dry reagent grade solvents were obtained from Merck (India) and further dried according to standard methods before use. Millipore water was used in all experiments.

2.2. Synthesis of SBA-15

A total of 4.4 g of tri block copolymer was dispersed in 40 mL distilled water and stirred for 2 h. The resultant solution was added to 120 g of 2 M HCl with stirring for 2 h. To this, 9.0 g of TEOS was added drop wise at room temperature with stirring for 24 h. The resulted mixture was subjected to hydrothermal treatment at 100˚C for 48 h under static condition. The solid obtained was filtered, washed with distilled water and dried in hot air oven at 60˚C for 12 h. The product was calcinated at 550˚C for 8 h in air to remove the template completely.

2.3. Synthesis of nanoporous silica SBA-15 Diaminocyclohexane derivative

One gram of SBA-15 was dissolved in 50 mL of toluene and to it 0.6 g 3-chloro propyl tri methoxy silane was added with stirring the reaction mixture at 90˚C for 24 h in N_2 atmosphere. The solid was filtered, washed with DCM and dried in oven at 60˚C for 12 h. The obtained compound was subjected to soxhlet extraction to remove the unreacted compounds. The product was dissolved in 100 mL of toluene and to it 1,2-diaminocyclohexane was added and refluxed for 24 h. The final product, diaminocyclohexane SBA-15 was collected after removal of solvent through filtration and drying in hot air oven at 60˚C for 12 h. The schematic mechanism of preparation of diaminocyclohexane SBA-15 is shown in Fig. 1.

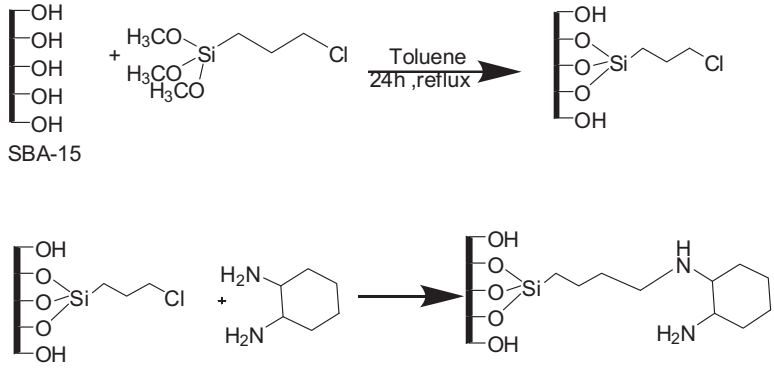

Fig. 1. Preparation of 1,2-diaminocyclohexane SBA-15.

2.4. Instruments

Powder XRD of the materials was recorded using a PANalytical X'pert Pro dual goniometer diffractometer. A proportional counter detector was used for low-angle experiments. The radiation used was Cu Kα (1.5418 Å) with a Ni filter and the data collection was carried out using a flat holder in Bragg-Brentano geometry (0.5°–5°; 0.2° min^{-1}). N_2 adsorption–desorption isotherms and pore size distributions were determined using a Micrometrics ASAP 2020 instrument and Autosorb 1C Quanta chrome (USA). HRTEM analysis of the samples was carried out using JEOL JEM-3010 and Tecnai (Model F30) microscopes operating at 300 kV. The textual structure of material was studied using a dual-beam scanning electron microscope (FEI, model Quanta 200 3D) operating at 30 kV. Infrared spectra of samples were recorded using a Perkin–Elmer (Spectrum one) FTIR spectrophotometer. For FTIR studies, the liquid samples or dilute solution of the solid samples in THF were spread over KBr pellets and their spectra were recorded. IR spectra were recorded in the range of 4,000–400 cm^{-1}. Thermal analysis (TGA–DTA) of the samples was carried out using a Pyris Diamond TGA analyzer with a heating rate of 10°C min^{-1} under air atmosphere. An Elico (LI-129) pH meter was used for pH measurements. The pH meter was calibrated using standard buffer solutions of pH 4.0, 7.0 and 9.2. The concentration of metal ions was determined using atomic absorption spectrometer (AA 6300, Shimadzu, Japan).

2.5. Batch adsorption experiments

Batch adsorption studies were performed by taking 50 mL of metal solution (pH 6.0) in a 100-mL flask and by adding 50 mg of Dach@SBA-15. The sealed flask was shaken at a speed of 300 rpm at temperature of 303 K by placing in a shaking incubator. After 3 h of shaking, adsorbent was separated by filtering through an ash less filter paper and the concentration of metal ions in solution was analysed by AAS. The influence of pH on Cu(II) and Ni(II) adsorption was studied by equilibrating the suspensions in solutions of different pH in the range of 2.0–7.0. The effect of contact time on adsorption of metal ions onto Dach@SBA-15 was studied by varying the contact time of suspensions from 5 to 70 min. For the adsorption isotherm studies, the initial metal ion concentration was varied over the range of 50–150 mg/L. The concentration of Dach@SBA-15 was varied between 50 and 150 mg in order to determine the required sorbate–sorbent ratio for optimum adsorption. The amount of metal ion sorbed onto the Dach@SBA-15, q_e, was computed by the following equation:

$$q_e = \frac{(C_i - C_e)V}{M} \tag{1}$$

where q_e (mg/g) is the equilibrium adsorption capacity of Cu(II) and Ni(II). C_i and C_e were initial and equilibrium concentrations (mg/L) of Cu(II) and Ni (II), respectively, M is the adsorbent dosage (mg) and V is the volume of the solution. The adsorption percentage was computed using the formula:

$$\text{Adsorption } (\%) = \frac{(C_i - C_e)}{C_i} \times 100 \tag{2}$$

3. Results and discussions

3.1. FT-IR analysis

FT-IR studies were used for characterizing the synthesized SBA-15 and assessing the anchoring of Dach onto the surface of SBA-15 and also for understanding the existence of surface functional groups which are

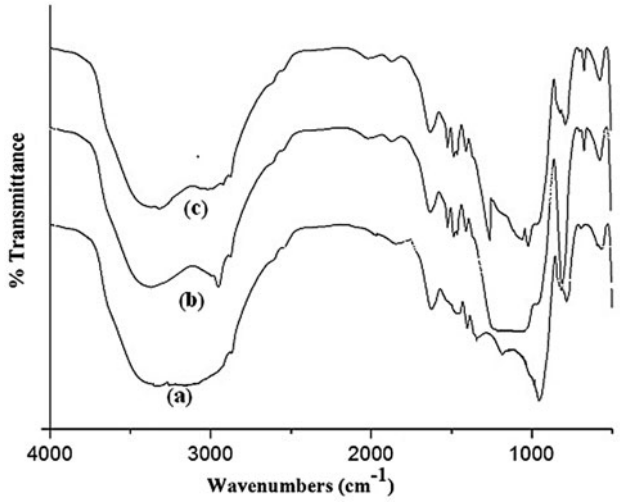

Fig. 2. FT-IR spectra of (a) calcinated SBA-15 (b) Dach@SBA-15 and (c) metal-chelated Dach@SBA-15.

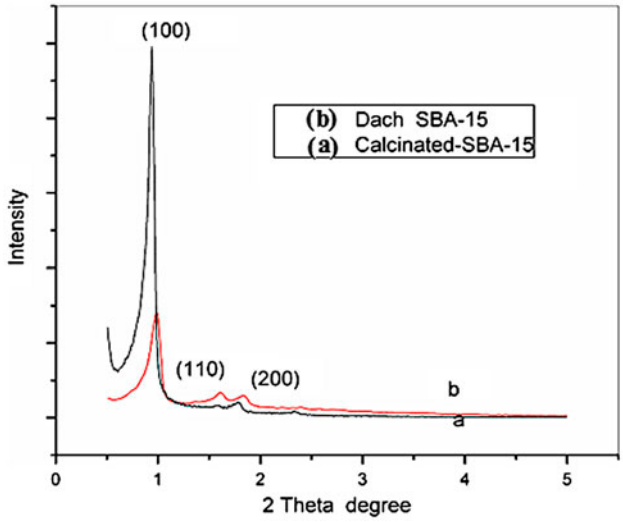

Fig. 3. XRD of (a) calcinated SBA-15 and (b) Dach@SBA-15.

responsible for metal ion binding. Fig. 2 represents the FT-IR spectra of SBA-15(2a), Dach@SBA-15 (2b) and metal-loaded Dach@SBA-15 (2c). In spectra of SBA-15, a broad band in the region of 3,450 cm^{-1} can be assigned to vibrational mode of silanol group (Si–OH) [28]. The band at 960 cm^{-1} is due to the Si–O stretching vibrations of Si–OH groups. The FT-IR spectra of Dach@SBA-15 (Fig. 2(b)) shows bands at 3,382 and 2,936 cm^{-1} which are due to the stretching mode of N–H and C–H groups, respectively. The band at 1,511 cm^{-1} represents the scissoring mode of NH_2. The deformation of CH_2–CH_3 was confirmed by the bands at 1,469 and 1,209 cm^{-1}. The C–N bands appeared at 1,092 and 1,209 cm^{-1} and the NH_2 and N–H wagging bands appeared between 660 and 900 cm^{-1} [29]. From spectra of Dach@SBA-15 (Fig. 2(b)) and metal-loaded Dach@SBA-15 (Fig. 2(c)), it is clear that band of N–H appeared at 3382 cm^{-1} in Fig. 2(b) is shifted to 3,320 cm^{-1} in Fig. 2(c), indicating the chelation of NH group to the metal ion.

3.2. Low-angle XRD and SEM analysis

Fig. 3(a) and (b) shows the low-angle XRD patterns of the calcinated SBA-15 and Dach@SBA-15 sorbent. The hexagonal structure of the compounds was indicated with characteristic of three peaks (100) (110) and (200). In the spectra of Dach@SBA-15, the intensity of peaks is decreased, which may be due to the attachment of organic functional groups in the nanoporous channels that reduced the scattering power of the nanoporous silicate wall. Fig. 4 shows the SEM images of calcinated SBA-15 and Dach@SBA-15 which indicate the well-distributed hexagonal particles arranged into rope-like sheet structure. The above results confirm the hexagonal and rope-like sheet structures to SBA-15 and Dach@SBA-15.

3.3. TEM analysis

The TEM and HRTEM studies of calcinated SBA-15 and Dach@SBA-15 were carried out to understand the structure and size of the prepared particles. TEM images of calcinated SBA-15 (Fig. 5(a)) and Dach@SBA-15 nanosheets (Fig. 5(c)) indicate the average diameter as 280 nm and length as above 650 nm for both the compounds. TEM image of Dach@SBA-15 (Fig. 5(c)) indicates that the nanosheet was slight changed because of interlinking of Dach ligands onto the surface of SBA-15. The HRTEM images of calcinated SBA-15 (Fig. 5(b)) and Dach@SBA-15 nanosheets (Fig. 5(d)) show that the compounds have porous structures.

3.4. TGA/DTA and elemental analysis

The thermal studies (TGA) of nanoporous silica were recorded in air atmosphere at heating rate of 10°C/m from 30 to 1,000°C. The TGA curves (Fig. 6) show that a degradation process occurred between 33 and 993°C with a total weight loss of about 54%. The data show three stages associated with the evaporation of excess H_2O molecules up to 100°C (stage I), loss of organic groups on SBA-15 (stage II) and the remaining inorganic matter (stage III). The organic content can be determined from the difference in weight loss between 100 and 700°C. The organic

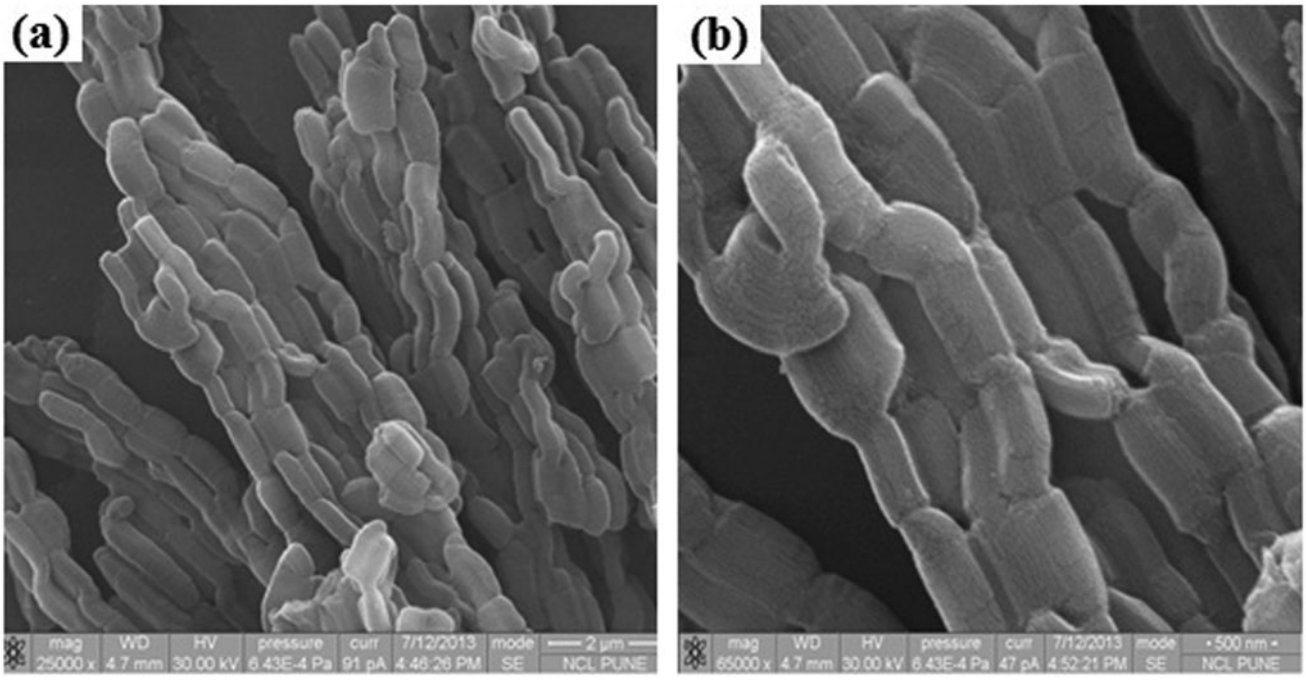

Fig. 4. SEM image of (a) calcinated SBA-15 and (b) Dach@SBA-15.

content in Dach@SBA-15 calculated for the hybrid material is relatively high (13.2 wt.%) which agrees with the value calculated by weight loss from TGA curves. Elemental analysis data of the Dach@SBA-15 (Table 1) indicates that the carbon and hydrogen contents increased on surface modification indicating the anchoring of organic functional groups onto SBA-15.

3.5. N_2 adsorption–desorption isotherms

The nitrogen adsorption–desorption isotherms of SBA-15 and Dach@SBA-15 (Fig. 7) displayed characteristic type IV isotherms (hysteresis) indicating the nanoporous structures which were not disturbed even after surface modification. The surface area and the pore size were calculated by BET and BJH methods and results are summarized in Table 2. As expected, the surface area, pore size and pore volume of SBA-15 were decreased on surface modification.

3.6. Effect of pH

The pH of solution is one of the most important variables that influence metal ion adsorption. The effect of pH on the removal of Cu(II) and Ni(II) ions by Dach@SBA-15 was investigated by varying the pH from 2.0 to 7.0 at 303 K. As shown in Fig. 8(a) and (b) the percentage removal of Cu(II) and Ni(II) increased with increase in pH from 2.0 to 6.0 and above that pH the percentage removal decreased with an increase in pH. Maximum removal (for Cu 98.1%, for Ni 96.8%) for both the metal ions was observed at pH 6.0 with an initial metal ion concentration of 50 mg/L. Decrease in metal ion removal at higher pH (pH > 6) may be because of the formation of hydroxyl ions of metals. Lower pH of the solution can affect the surface charge of Dach@SBA-15, which impact the adsorption of metal ions on the surface of the Dach@SBA-15. Nevertheless, at higher pH, electrostatic attraction increases between the surface functional groups and metal ions so it increases adsorption capacity.

3.7. Adsorption kinetics

Fig. 9(a) and (b) show the adsorption behaviour of Cu(II) and Ni(II) onto the Dach@SBA-15 at initial concentration of 50 mg/L, pH 6.0 at 303 K as a function of contact time. The adsorption rate of the Cu(II) and Ni(II) onto Dach@SBA-15 was gradually increased and reached equilibrium in 60 min. The pseudo-first-order [30,31] and pseudo-second-order [32] kinetic models were used to investigate the kinetics of removal of metal ions by Dach@SBA-15.

The linear form of pseudo-first-order kinetic model is described by the equation:

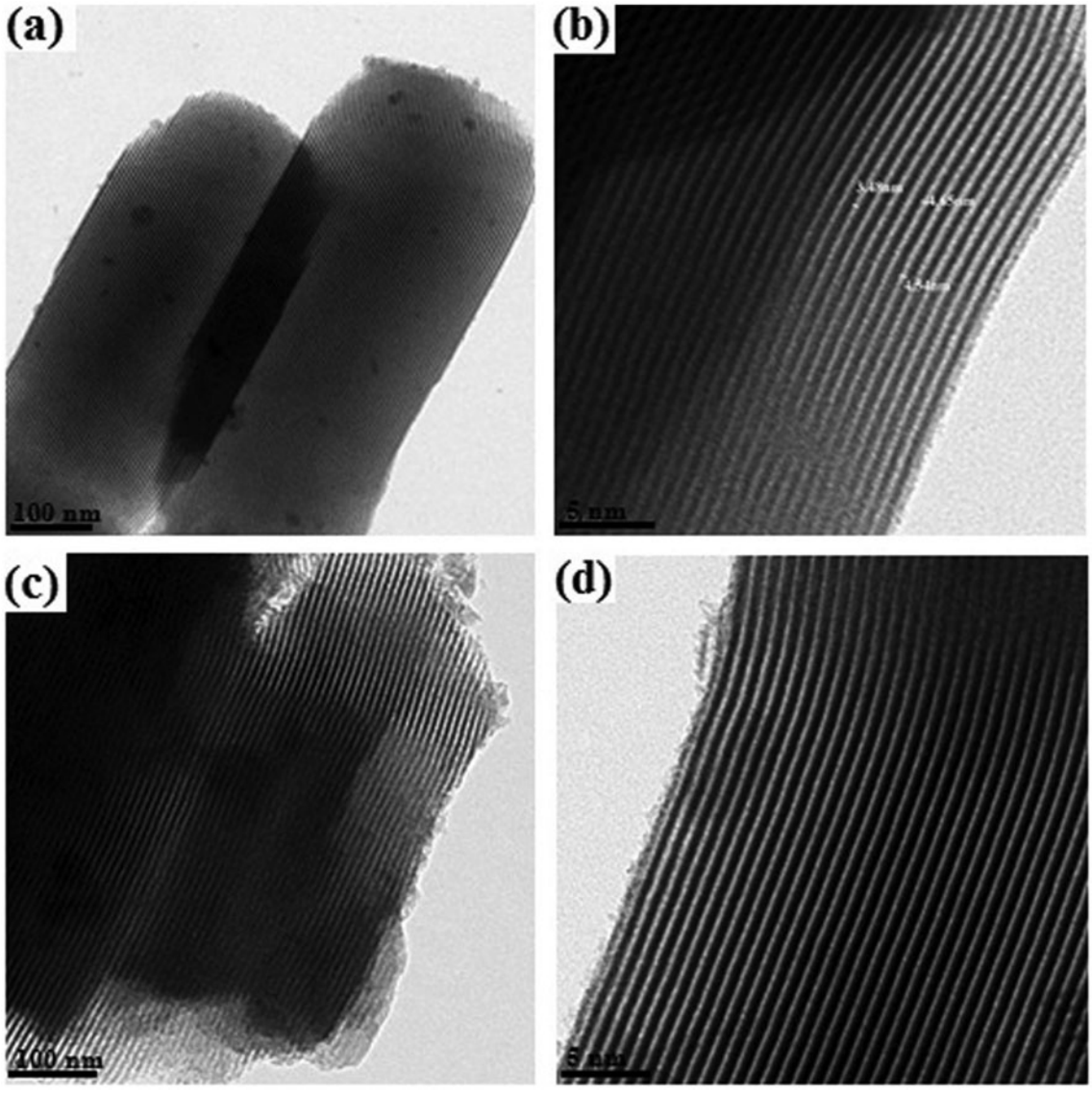

Fig. 5. TEM and HRTEM images of (a) calcinated SBA-15 and (b) Dach@SBA-15.

$$\log(q_e - q_t) = \log q_e - \left(\frac{k_1}{2.303}\right)t \quad (3)$$

where k_1 (min^{-1}) is the pseudo-first-order rate constant of adsorption, q_e (mg/g) and q_t (mg/g) are the amount of the Cu(II) and Ni(II) adsorbed at equilibrium and at time t. The pseudo-first-order kinetic constant were determined from slope of the plot of log ($q_e - q_t$) vs. t. The R^2 value is very less suggesting that the adsorption of Cu(II) and Ni(II) ions does not follow pseudo-first-order kinetic model (Data were not shown). The kinetic data were further analysed using pseudo-second-order kinetic model. The linearized form of the equation is represented as:

$$\frac{t}{q_t} = \frac{1}{k_2 q_e^2} + \left(\frac{1}{q_e}\right)t \quad (4)$$

where k_2 (g/mg/min) is the pseudo-second-order rate constant, q_e (mg/g) and q_t (mg/g) are the amount of the Cu(II) and Ni(II) adsorbed at equilibrium and at time t. The values of k_2 and q_e can be calculated from the slope and intercept of a plot of t/q_t vs. t. From the removal kinetics shown in Fig. 10(a) and (b), the slope show good linearity with the correlation coefficient value (R^2) of 0.9999 for Cu(II) and 0.9999 for Ni(II) indicating that the removal kinetics follow the pseudo-second-order model. The corresponding parameters of the pseudo-second-order kinetics are listed in Table 3.

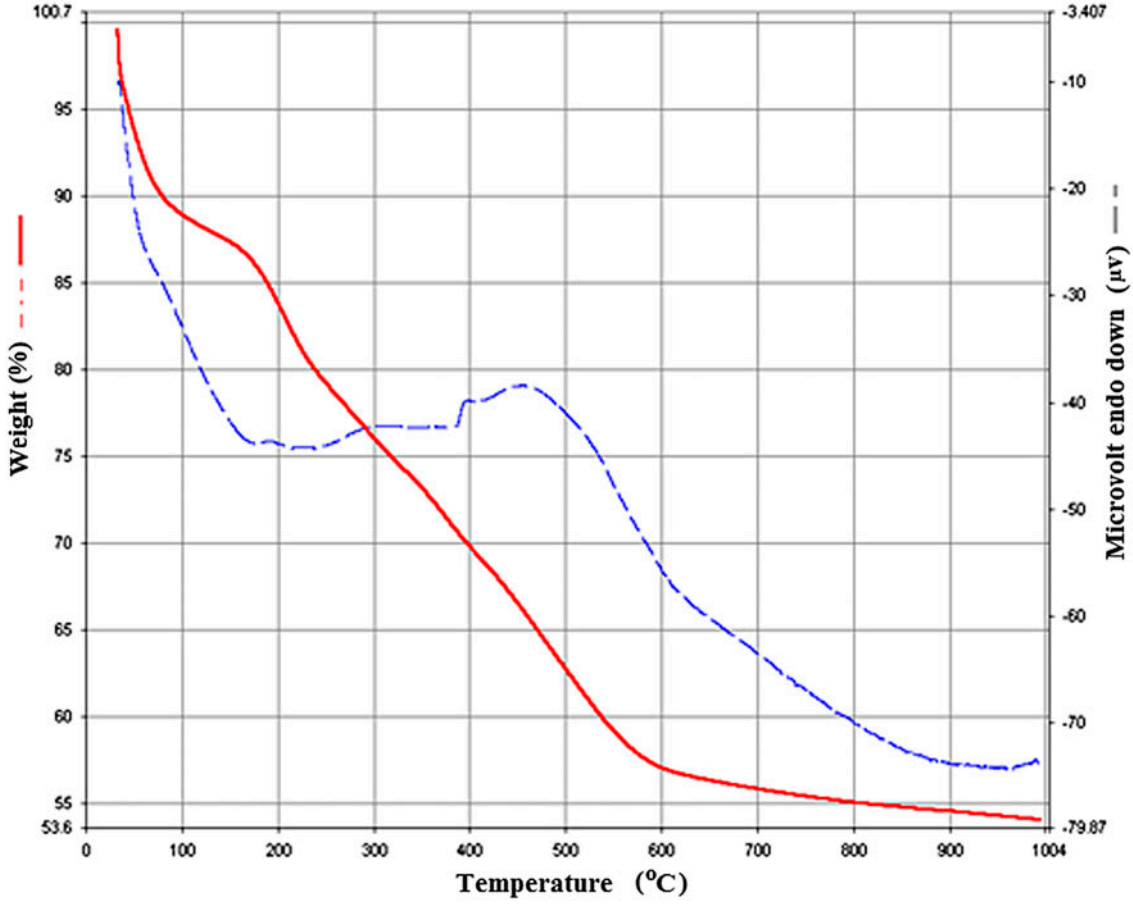

Fig. 6. TGA/DTA of Dach@SBA-15 nanoporous silica.

Table 1
(1) SBA-15-Cl and (2) modified organic functional group Dach@SBA-15

S.No	Compound	% Carbon	% Nitrogen	% Hydrogen	% Sulphur
1	SBA-15-Cl	4.63	–	1.10	–
2	Dach@SBA-15	14.18	3.27	3.16	–

The adsorption system obeyed the pseudo-second-order kinetics for the entire adsorption period and thus supported the assumption of adsorption was a chemisorptions process [33].

3.8. Adsorption isotherm

To evaluate the maximum adsorption capacity of adsorbent and the equilibrium adsorption of Ni(II) and Cu(II) onto Dach@SBA-15, the adsorption data were analysed by the Langmuir and Freundlich isotherm models. The Langmuir equation can be expressed by the linearized form:

$$\frac{C_e}{q_e} = \frac{C_e}{q_m} + \frac{1}{q_m b} \tag{5}$$

where q_e is the equilibrium adsorption capacity of metal ion concentration onto the adsorbent (mg/g), C_e is the equilibrium metal ion concentration in the solution (mg/L), q_m is the maximum capacity of adsorbent (mg/g) and b (L/mg) is the equilibrium constant relating to the sorption energy. Fig. 11(a) and (b) shows that the experimental data fits the Langmuir adsorption isotherm well with maximum adsorption capacity of 90.09 and 84.03 mg/g for Cu(II) and Ni(II)

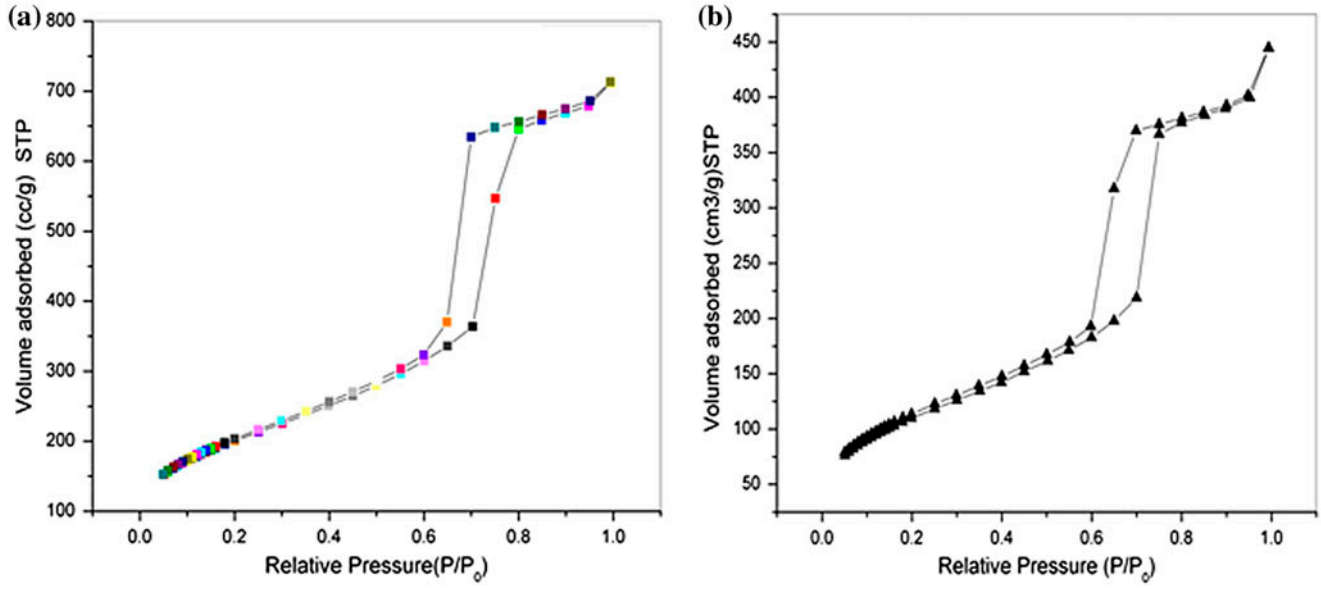

Fig. 7. (a, b) Nitrogen adsorption–desorption isotherms of calcinated SBA-15 and Dach@SBA-15.

Table 2
Calcinated SBA-15 and modified SBA-15 for the surface area, pore volume and pore radius

Materials	Surface area (m/g)	Pore volume (cc/g)	Pore radius (Å)
SBA-15	607.488	1.024	32.731
Dach@SBA-15	394.506	0.662	28.037

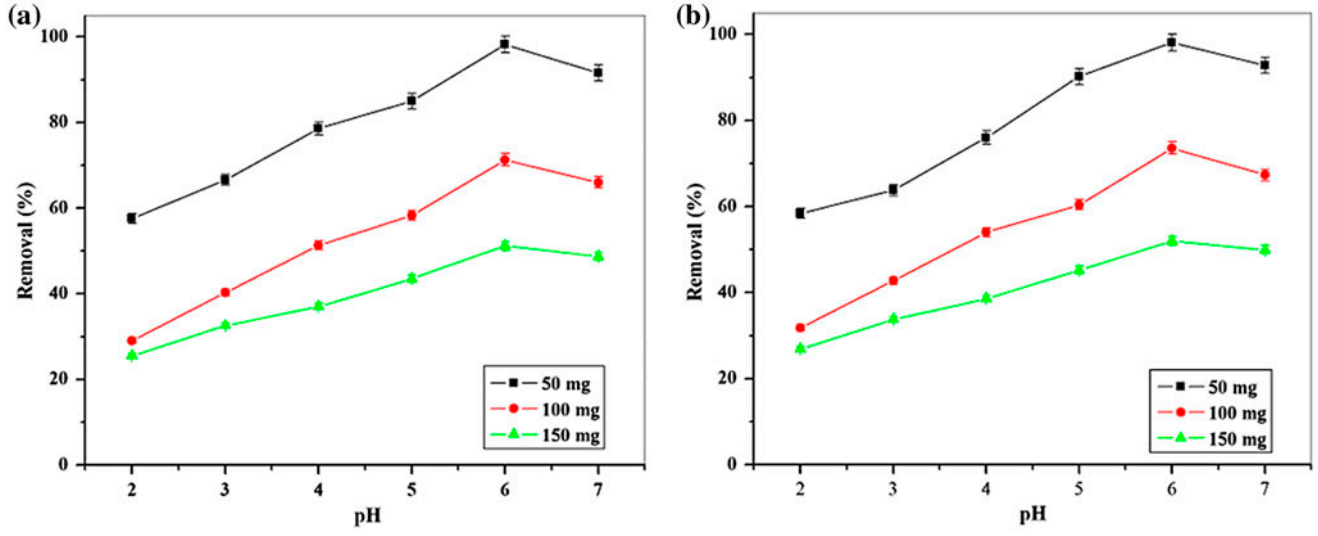

Fig. 8. (a, b) Effect of pH on the adsorption of Cu(II) and Ni(II) by Dach@SBA-15 at different initial concentrations (initial concentrations of Cu(II) and Ni(II): 50, 100, 150 mg/L, material dosage: 0.5 g/L, solution volume: 50 m/L, time: 120 min, temperature: 303 K).

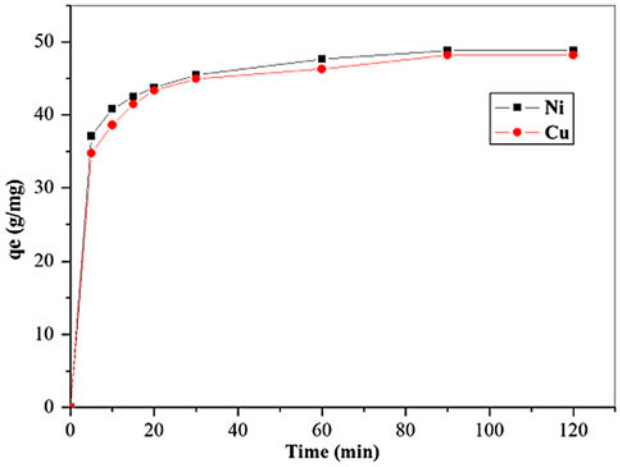

Fig. 9. (a, b) Effect of contact time on the adsorption of Cu (II)) and Ni(II) by Dach@SBA-15 (initial concentration of Cu(II) and Ni(II) 50 mg/L, material dosage: 0.5 g/L, solution volume: 50 mL, pH 6.0, temperature: 303 K).

respectively. The correlation coefficients and equilibrium constants are summarized in Table 4. In addition, another parameter in the Langmuir adsorption isotherm, a dimensionless factor (R_L) is described by the following equation.

$$R_L = \frac{1}{1 + bC_i} \tag{6}$$

where C_i (mg/g) is initial metal concentration, b (L/mg) is the Langmuir constant. For favourable sorption, $0 < R_L < 1$; for unfavourable sorption, $R_L > 1$; for irreversible sorption $R_L < 0$; for linear sorption, $R_L < 1$. In this study, the R_L values are 0.0467 and 0.0647, which lies between 0 and 1. This indicates that the adsorption of Cu(II) and Ni(II) onto Dach@SBA-15 is favourable. The Freundlich isotherm is applicable for modelling the adsorption of metal ions on heterogeneous surfaces and the linearized form of isotherm is expressed as:

$$\log q_e = \log k_f + \frac{1}{n} \log C_e \tag{7}$$

where K_f (mg/g) and "n" are the Freundlich isotherm constants that represents the adsorption and the intensity of adsorbents, Fig. 12(a) and (b) shows the linear plot of Freundlich isotherms of Cu(II) and Ni(II) onto Dach@SBA-15 at 303 K. The fitted constants for the

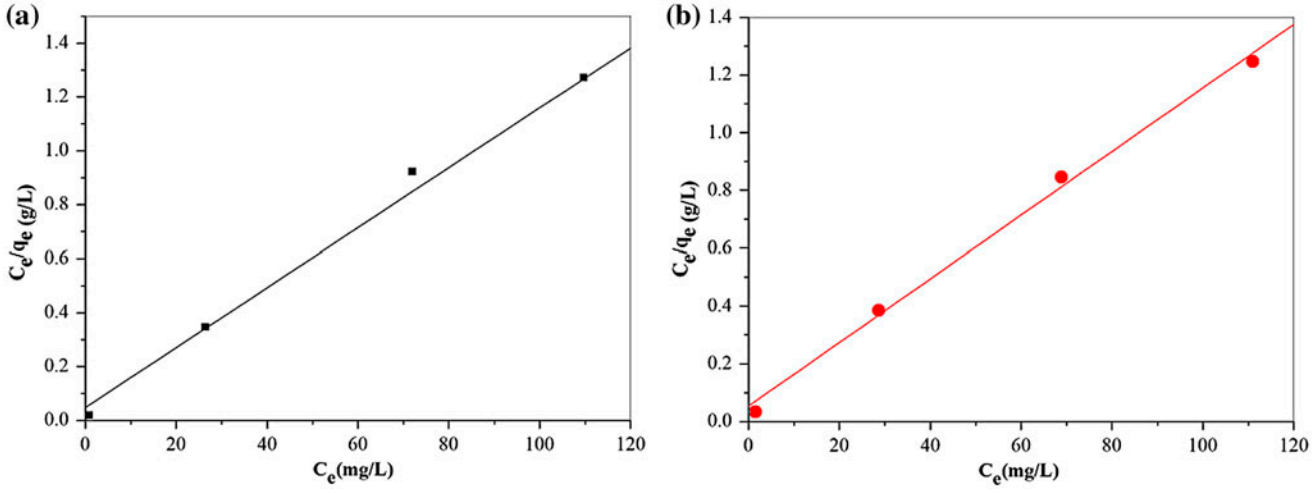

Fig. 10. (a, b) Linear plot of Langmuir isotherm of Cu(II) and Ni(II) onto Dach@SBA-15 silica.

Table 3
Kinetic parameters of pseudo-second-order models for the adsorption of Cu(II) and Ni(II) on Dach@SBA-15 silica sorbent

Pseudo-second-order				
	$q_{e,exp}$ (mg/g)	k_2 (g/mg/min)	$q_{e,cal}$ (mg/g)	R^2
Cu(II)	48.79	0.0094	49.75	0.9999
Ni(II)	48.20	0.0073	49.50	0.9999

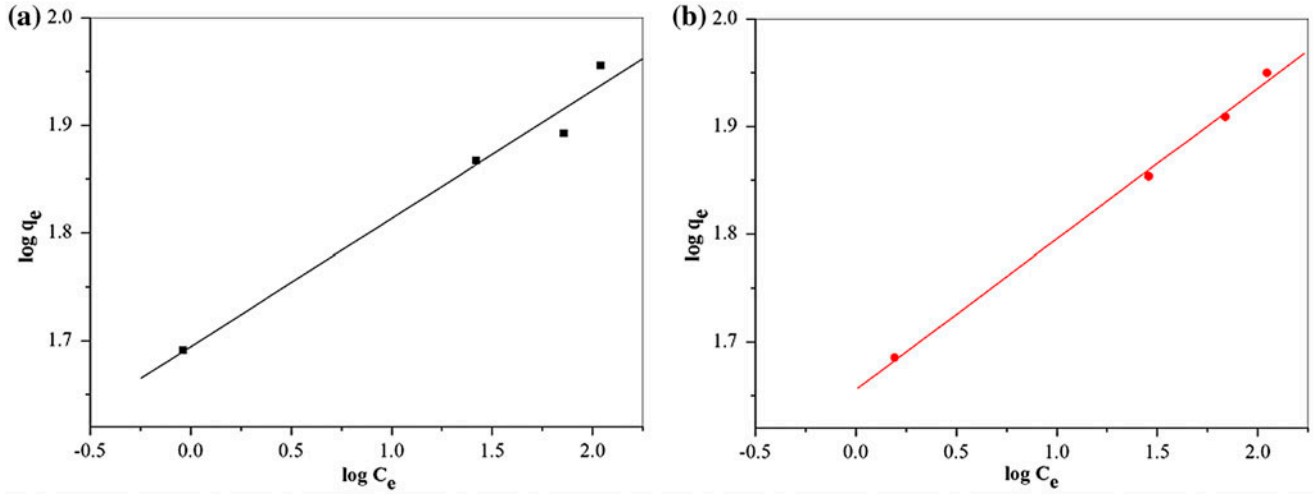

Fig. 11. (a, b) Linear plot of Freundlich isotherm of Cu(II) and Ni(II) onto Dach@SBA-15 silica.

Table 4
Langmuir and Freundlich isotherm constants

	Langmuir			Freundlich		
	q_m (mg/g)	b (L/mg)	R^2	k_f (mg/g)	n	R^2
Cu(II)	90.09	0.2890	0.9981	49.4652	8.4104	0.9884
Ni(II)	84.03	0.4075	0.9982	45.1128	7.1073	0.9746

Freundlich isotherm model, K_f, "n" and correlation coefficient (R^2) are calculated from the intercept and slope of the plot and are presented in Table 4. The values of $n > 1$ represent favourable adsorption condition [34,35] and the "n" values for Cu(II) is 8.41 and for Ni (II) is 7.11. These values suggest that the Dach@SBA-15 is a good sorbent for the adsorption of Cu(II) and Ni (II) ions. The adsorption data fit well to Langmuir model and have similar correlation coefficients. This may be attributed to a good anchoring of Dach on SBA-15 nanoporous silica, and the uniform distribution of active sites for metal ion adsorption with monolayer

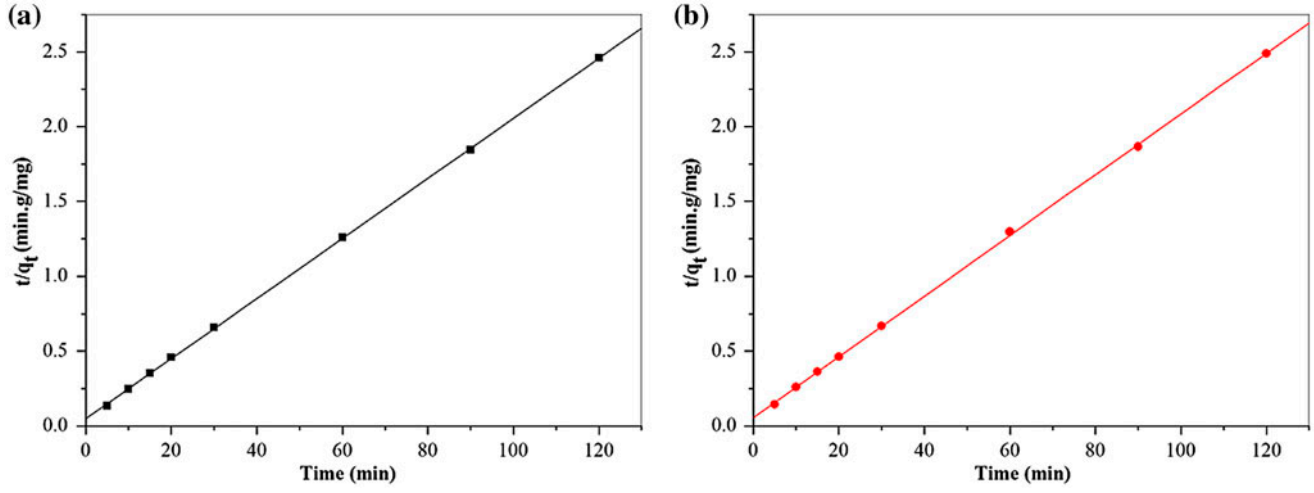

Fig. 12. (a, b) Pseudo second-order adsorption kinetics of Cu(II) and Ni(II) onto Dach@SBA-15 silica.

Table 5
Comparison of adsorption capacities with different adsorbents

Type of adsorbents	Capacity (mg/g)	Refs.
EDTA modified SBA-15	13.2	[36]
Magnetic hydrogels	126.40	[37]
Multiwall carbon nanotubes/Fe_3O_4-NH_2	75.02	[38]
Aminopropyl MCM-41	30.5	[39]
Mercacaptopropyl -functionalized porous silica	13	[40]
Dach@SBA-15 silica sorbent	84–90	This work

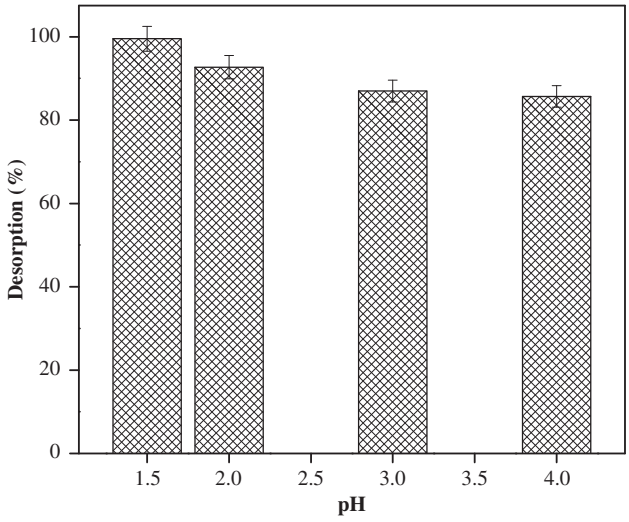

Fig. 13. Desorption of Cu(II) and Ni(II) with HCl at different pH.

coverage. The adsorption capacity values of Dach@SBA-15 for Cu(II) and Ni(II) from Langmuir isotherm model were compared with that of various adsorbents and are given in Table 5.

3.9. Desorption and reusability

Due to the economic efficiency and environmental sustainability, it is essential for regeneration and reuse of an adsorbent. From the pH study, the adsorption percentage for Cu(II) and Ni(II) was lower at lower pH. Hence, acidic medium is expected to be a feasible approach for the regeneration of Cu(II)- and Ni(II)-loaded Dach@SBA-15. Thus, dilute HCl solutions of different pH were used to study the desorption of metal ions from Dach@SBA-15 and results are presented in Fig. 13. It was found that the desorption percentage values were 99.52, 92.70, 87.00 and 85.68% with HCl solutions of pH 1.5, 2.0, 3.0 and 4.0, respectively. At lower pH, higher desorption was observed because of the sufficiently high hydrogen ion concentration, which led to the strong competitive adsorption. The results indicate that the Dach@SBA-15 can be reused for removal of Cu(II) and Ni(II).

4. Conclusion

A new hybrid sorbent, Dach@SBA-15 was prepared, characterized and used for the removal Cu(II) and Ni(II) from aqueous media. The surface of the silica was modified by anchoring with 1,2-diaminocyclohexane onto SBA-15. TEM image shows that SBA-15and Dach@SBA-15 contain sheet-like structure. Nanoporous property of the sorbent was confirmed by XRD analysis and FT-IR results revealed the surface functional groups of Dach@SBA-15. The maximum adsorption of Cu(II) and Ni(II) onto Dach@SBA-15 was observed at pH 6.0 with maximum adsorption capacity values of 90.09 for Cu(II) and 84.03 mg/g for Ni(II) at 303 K. Desorption studies with HCl revealed that Dach@SBA-15 can be regenerated by treatment with HCl and can be reused as the sorbent for several cycles.

Acknowledgements

The authors are thankful to the DST, New Delhi for providing financial assistance (Grant No: SR/S1/IC-63/2012). The authors are also thankful to National Chemical Laboratory; Pune, India for providing instrument facility.

References

[1] S.-M. Lee, C. Laldawngliana, D. Tiwari, Iron oxide nano-particles-immobilized-sand material in the treatment of Cu(II), Cd(II) and Pb(II) contaminated waste waters, Chem. Eng. J. 195–196 (2012) 103–111.
[2] N.A.A. Babarinde, J.O. Babalola, R.A. Sanni, Biosorption of lead ions from aque-ous solution by maize leaf, Int. J. Phys. Sci. 1 (2006) 23–26.
[3] A.N. Kursunlu, E. Guler, H. Dumrul, O. Kocyigit, I.H. Gubbuk, Chemical modification of silica gel with synthesized new Schiff base derivatives and sorption

studies of cobalt(II) and nickel(II), Appl. Surf. Sci. 255 (2009) 8798–8803.
[4] H. Dumrul, A. Kursunlu, O. Kocyigit, E. Guler, S. Ertul, Adsorptive removal of Cu(II) and Ni(II) ions from aqueous media by chemical immobilization of three different aldehydes, Desalination 271 (2011) 92–99.
[5] A. Çimen, A. Bilgiç, A.N. Kursunlu, İ.H. Gübbük, H.I. Uçan, Adsorptive removal of Co(II), Ni(II), and Cu(II) ions from aqueous media using chemically modified sporopollenin of Lycopodium clavatum as novel biosorbent, Desalin. Water Treat. 52 (2014) 4837–4847.
[6] WHO, Guidelines for drinking water quality, health criteria and other supporting information, WHO, Geneva, 973 1996.
[7] M.H. Kalavathy, T. Karthikeyan, S. Rajgopal, L.R. Miranda, Kinetic and isotherm studies of Cu(II) adsorption onto H3PO4-activated rubber wood sawdust, J. Colloid Interface Sci. 292 (2005) 354–362.
[8] V.O. Arief, K. Trilestari, J. Sunarso, N. Indraswati, S. Ismadji, Recent progress on biosorption of heavy metals from liquids using low cost biosorbents: Characterization, biosorption parameters and mechanism studies, Clean Soil Air Water 36(12) (2008) 937–962.
[9] F. Fu, Q. Wang, Removal of heavy metal ions from wastewaters: A review, J. Environ. Manage. 92 (2011) 407–418.
[10] B. Alyüz, S. Veli, Kinetics and equilibrium studies for the removal of nickel and zinc from aqueous solutions by ion exchange resins, J. Hazard. Mater. 167 (2009) 482–488.
[11] L.F. Greenlee, D.F. Lawler, B.D. Freeman, B. Marrot, P. Moulin, Reverse osmosis desalination: Water sources, technology, and today's challenges, Water Res. 43 (2009) 2317–2348.
[12] M.A. Barakat, E. Schmidt, Polymer-enhanced ultrafiltration process for heavy metals removal from industrial wastewater, Desalination 256 (2010) 90–93.
[13] P.S. Sudilovskiy, G.G. Kagramanov, V.A. Kolesnikov, Use of RO and NF for treatment of copper containing wastewaters in combination with flotation, Desalination 221 (2008) 192–201.
[14] T.A. Kurniawan, G.Y.S. Chan, W.H. Lo, S. Babel, Physico-chemical treatment techniques for wastewater laden with heavy metals, Chem. Eng. J. 118 (2006) 83–98.
[15] L. Zhang, W. Zhang, J. Shi, Z. Hua, Y. Li, J. Yan, A new thioether functionalized organic– inorganic mesoporous composite as a highly selective and capacious Hg^{2+} adsorbent, Chem. Commun. (2003) 210–211.
[16] X. Ren, D. Shao, S. Yang, J. Hu, G. Sheng, X. Tan, X. Wang, Comparative study of Pb(II) sorption on XC-72 carbon and multi-walled carbon nanotubes from aqueous solutions, Chem. Eng. J. 170(1) (2011) 170–177.
[17] K.S. Hui, C.Y.H. Chao, S.C. Kot, Removal of mixed heavy metal ions in wastewater by zeolite 4A and residual products from recycled coal fly ash, J. Hazard. Mater. 127 (2005) 89–101.
[18] L.Y. Wang, L.Q. Yang, Y.F. Li, Y. Zhang, X.J. Ma, Z.F. Ye, Study on adsorption mechanism of Pb(II) and Cu (II) in aqueous solution using PS-EDTA resin, Chem. Eng. J. 163 (2010) 364–372.
[19] Y. Xu, J. Zhang, G. Qian, Z. Ren, Z.P. Xu, Y. Wu, Q. Liu, S. Qiao, Effective Cr(VI) removal from simulated groundwater through the hydrotalcite-derived adsorbent, Ind. Eng. Chem. Res. 49 (2010) 2752–2758.
[20] M.A. Martín-Lara, I.L. Rodríguez, G. Blázquez, M. Calero, Factorial experimental design for optimizating the removal conditions of lead ions from aqueous solutions by three wastes of the olive-oil production, Desalination 278 (2011) 132–140.
[21] A.K. Bhattacharya, S.N. Mandal, S.K. Das, Adsorption of Zn(II) from aqueous solution by using different adsorbents, Chem. Eng. J. 123 (2006) 43–51.
[22] I. Villaescusa, N. Fiol, M. Martínez, N. Miralles, J. Poch, J. Serarols, Removal of copper and nickel ions from aqueous solutions by grape stalks wastes, Water Res. 38 (2004) 992–1002.
[23] M. Machida, B. Fotoohi, Y. Amamo, L. Mercier, Cadmium(II) and lead(II) adsorption onto hetero-atom functional mesoporous silica and activated carbon, Appl. Surf. Sci. 258 (2012) 7389–7394.
[24] K.S. Abou-El-Sherbini, I.M.M. Kenawy, M.A. Hamed, R.M. Issa, R. Elmorsi, Separation and preconcentration in a batch mode of Cd(II), Cr(III, VI), Cu(II), Mn(II, VII) and Pb(II) by solid-phase extraction by using of silica modified with Npropylsalicylaldimine, Talanta 58 (2002) 89–300.
[25] M. Mureseanu, A. Reiss, I. Stefanescu, E. David, V. Parvulescu, G. Renard, V. Hulea, Modified SBA-15 mesoporous silica for heavy metal ions remediation, Chemosphere 73 (2008) 1499–1504.
[26] H. Yang, R. Xu, X. Xue, F. Li, G. Li, Hybrid surfactant-templated mesoporous silica formed in ethanol and its application for heavy metal removal, J. Hazard. Mater. 152 (2008) 690–698.
[27] Y. Jiang, Q. Gao, H. Yu, Y. Chen, F. Deng, Intensively competitive adsorption for heavy metal ions by PAMAM-SBA-15 and EDTA-PAMAM-SBA-15 inorganic–organic hybrid materials, Microporous Nanoporous Mater. 103 (2007) 316–324.
[28] K. Nakamoto, Infrared and Raman spectra of inorganic and coordination compounds, John wiley, New York, NY 2009.
[29] D. Jiang, J. Gao, J. Yang, W. Su, Q. Yang, C. Li, Mesoporous ethane-silicas functionalized with trans-(1R,2R)-diaminocyclohexane: Relation between structure and catalytic properties in asymmetric transfer hydrogenation, Microporous Mesoporous Mater. 105 (2007) 204–210.
[30] S. Lagergren, Zur theorie der sogenannten adsorption gelsterstoffe (On the theory of so-called adsorption of dissolved substances), Kungliga S venska Vetenskapsakademiens Seven Vetenskapsakad, Handlinger 24 (1898) 1–39.
[31] Z.Y. Yao, J.H. Qi, L.H. Wang, Equilibrium, kinetic and thermodynamic studies on the biosorption of Cu(II) onto chestnut shell, J. Hazard. Mater. 174 (2010) 137–143.
[32] Y.S. Ho, G. McKay, Pseudo-second order model for sorption processes, Process Biochem. 34 (1999) 451–465.
[33] G. Crini, H.N. Peindy, F. Gimbert, C. Robert, Removal of C.I. Basic Green 4 (Malachite Green) from aqueous solutions by adsorption using cyclodextrin-based adsorbent: Kinetic and equilibrium studies, Sep. Purif. Technol. 53 (2007) 97–110.

[34] B.H. Hameed, D.K. Mahmoud, A.L. Ahmad, Equilibrium modeling and kinetic studies on the adsorption of basic dye by a low-cost adsorbent: Coconut (*Cocos nucifera*) bunch waste, J. Hazard. Mater. 158 (2008) 65–72.
[35] J. Gong, T. Liu, X. Wang, X. Hu, L. Zhang, Efficient removal of heavy metal ions from aqueous systems with the assembly of anisotropic layered double hydroxide nanocrystals@carbon nanosphere, Environ. Sci. Technol. 45 (2011) 6181–6187.
[36] Y. Jiang, Q. Gao, H. Yu, Y. Chen, F. Deng, Intensively competitive adsorption for heavy metal ions by PAMAM-SBA-15 and EDTA-PAMAM-SBA-15 inorganic–organic hybrid materials, Microporous Mesoporous Mater. 103 (2007) 316–324.
[37] O. Ozay, S. Ekici, Y. Baran, N. Aktas, N. Sahiner, Removal of toxic metal ions with magnetic hydrogels, Water Res. 43 (2009) 4403–4411.
[38] L. Ji, L. Zhou, X. Bai, Y. Shao, G. Zhao, Y. Qu, C. Wangand, Y. Li, Facile synthesis of multiwall carbon nanotubes/iron oxides for removal of tetrabromobisphenol A and Pb(II), J. Mater. Chem. 22 (2012) 15853–15862.
[39] M. Algarra, M.V. Jiménez, E.R. Rodríguez-Castellón, A.J. Jiménez-López, J.J. Jiménez-Jiménez, Heavy metals removal from electroplating wastewater by aminopropyl-Si MCM- 41, Chemosphere 59 (2005) 779–786.
[40] B. Lee, Y. Kim, H. Lee, J. Yi, Synthesis of functionalized porous silicas via templating method as heavy metal ion adsorbents: the introduction of surface hydrophilicity onto the surface of adsorbents, Microporous Mesoporous Mater. 50 (2001) 77–90.